 Human Molecular Genetics, 2002, Vol. 11, No. 25 3135–3144

The Bloom syndrome helicase BLM interacts with TRF2 in ALT cells and promotes telomeric DNA synthesis

Dimitrios J. Stavropoulos[1,2], Paul S. Bradshaw[1,2], Xiaobin Li[2], Ivan Pasic[1,2], Kevin Truong[3,4], Mitsuhiko Ikura[3,4], Mark Ungrin[3] and M. Stephen Meyn[1,2,5,*]

[1]Department of Molecular and Medical Genetics, University of Toronto, Toronto, Canada M5S 1A8,
[2]Genetics and Genomic Biology Program, Hospital for Sick Children, Toronto, Canada M5G 1X8,
[3]Department of Medical Biophysics, University of Toronto, Toronto, Canada M5G 2M9,
[4]Division of Molecular and Structural Biology, Ontario Cancer Institute, Toronto, Canada M5G 2M9 and
[5]Department of Pediatrics, University of Toronto, Toronto, Canada M5G 1X8

Received July 26, 2002; Revised and Accepted October 7, 2002

Telomerase-negative immortalized human cells maintain telomeres by alternative lengthening of telomeres (ALT) pathway(s), which may involve homologous recombination. We find that endogenous BLM protein co-localizes with telomeric foci in ALT human cells but not telomerase positive immortal cell lines or primary cells. BLM interacts *in vivo* with the telomeric protein TRF2 in ALT cells, as detected by FRET and co-immunoprecipitation. Transient over-expression of green fluorescent protein (GFP)-BLM results in marked, ALT cell-specific increases in telomeric DNA. The association of BLM with telomeres and its effect on telomere DNA synthesis require a functional helicase domain. Our results identify BLM as the first protein found to affect telomeric DNA synthesis exclusively in human ALT cells and suggest that BLM facilitates recombination-driven amplification of telomeres in ALT cells.

INTRODUCTION

While the majority of human tumors and immortalized cell lines maintain their telomeres by activation of the reverse-transcriptase telomerase (1–3), ~10% of human tumors lack detectable telomerase activity and maintain their telomeres via the alternative lengthening of telomeres (ALT) pathway (4–7). The ALT pathway in human cells is associated with marked increases in telomere length variance, presence of extra-chromosomal telomeric DNA repeats (ECTR) and rapid telomere lengthening and deletion events of several kilobases (4,5,8–10).

Activation of the ALT pathway in *Saccharomyces cerevisiae* depends on Rad52 (11), a protein required for mitotic homologous recombination (12). The *S. cerevisiae* ALT pathway has been further divided into the Rad51-dependent type I, which is characterized by multiple tandem copies of the sub-telomeric Y′ element and very short $C_{1-3}A/TG_{1-3}$ tracts; and the Rad50-dependent type II, which has very heterogeneous and long telomeric repeat tracts, a telomere length profile reminiscent of human ALT tumors and cell lines (13,14). The proteins required for the human ALT pathway of telomere maintenance have not been identified. However, it has been shown that telomeric DNA and the telomeric proteins, TRF1 and TRF2 co-localize with the recombination proteins hRAD51 and hRAD52 as well as NBS1 in promyelocytic leukemia (PML) bodies in human ALT cell lines and tumors (15,16). PML bodies are 0.1–1 μm diameter nuclear matrix-associated structures of unknown function that contain PML protein (17) and have been proposed to play a role in a wide range of cellular processes including oncogenesis, apoptosis and repair of DNA damage (18–23). In addition, it has recently been demonstrated that DNA sequences are copied from one telomere to another in human ALT cells (24). These observations suggest that the human ALT pathway, like ALT in *S. cerevisiae*, may involve homologous recombination (11,13,14).

BLM is a RecQ helicase (25) that is involved in homologous recombination (26–29), can migrate Holliday junctions (30) and unwind G4-DNA (31), which forms *in vitro* at G-rich sequences such as telomeres. Mutations in *BLM* cause Bloom syndrome, a rare inherited disorder characterized by growth retardation, immunodeficiency, cancer and chromosomal instability (32). In human somatic cells, BLM protein

*To whom correspondence should be addressed at: Genetics and Genome Biology Program, Hospital for Sick Children, 11-101 Elm Wing, Toronto, 555 University Ave, Toronto, Canada M5G 1X8. Tel: +1 4168138485; Fax: +1 4168134931; Email: meyn@sickkids.ca

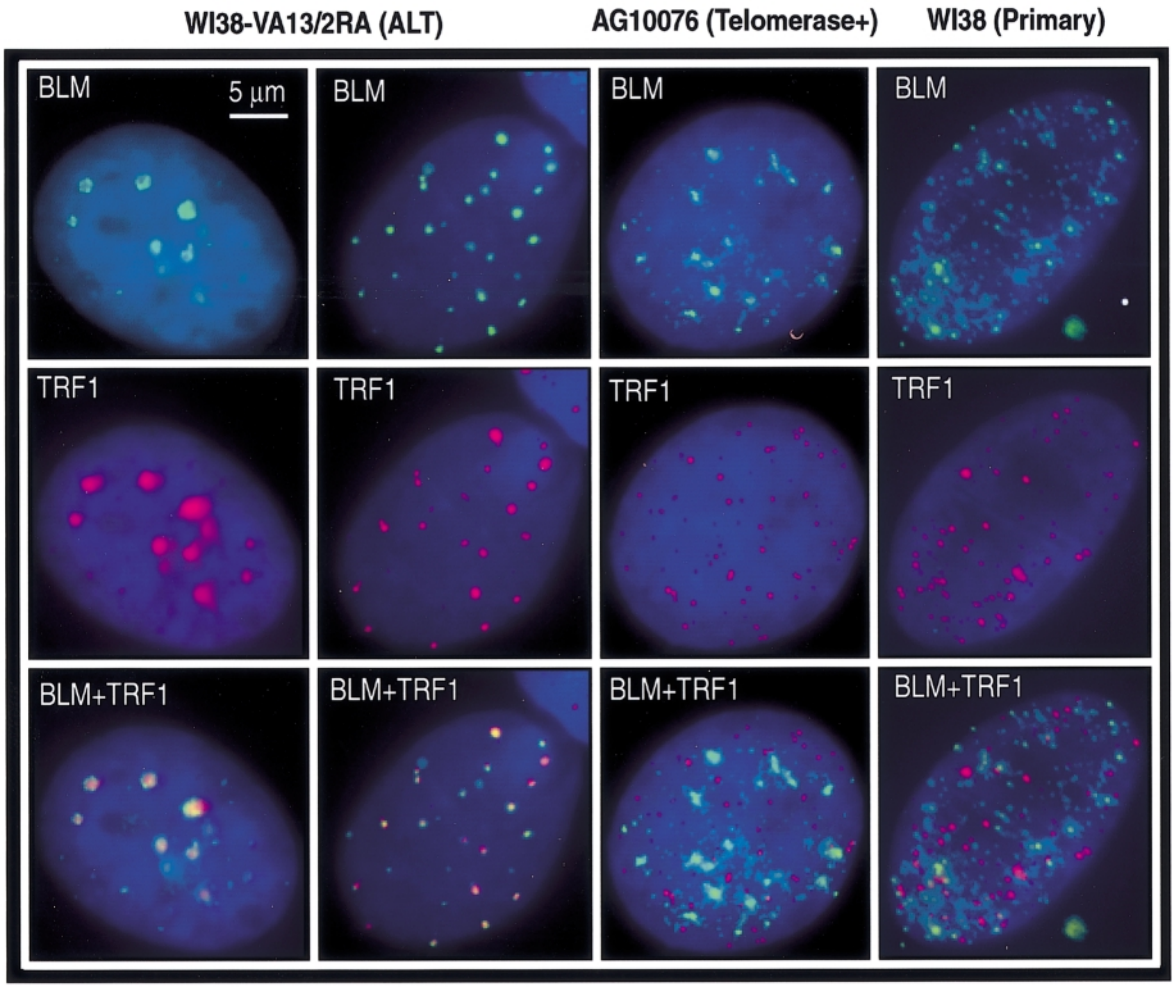

Figure 1. Co-localization between BLM and telomeric foci in ALT but not telomerase positive or primary cells. Cells were stained with DAPI (blue), mouse anti-BLM (green) and rabbit anti-TRF1 (red) antibodies. The BLM antibodies did not stain the nuclei of BLM mutant cell line GM08505B and we confirmed that rabbit anti-TRF1 antibodies represent telomeric foci by hybridizing interphase cells with a telomere sequence-specific peptide nucleic acid (PNA) probe and staining with the rabbit anti-TRF1 antibody (not shown). Co-localization between BLM and TRF1 was confirmed with rabbit anti-BLM and mouse anti-TRF1 antibodies (not shown). Cells with greater than 50% of foci overlapping were scored as positive for significant co-localization. According to these criteria, no co-localization was observed in two telomerase-positive (GM00639 and AG10076) and primary cell lines (WI38 and GM01161). Notice that BLM foci co-localize with large aggregates of TRF1, which are characteristic of ALT cell lines and tumors (15), as well as smaller TRF1 foci in WI38-VA13/2RA.

co-localizes with PML bodies (21,33,34) and the BLM protein was recently shown to co-localize with telomeric foci in a human ALT cell line (33). However, the potential involvement of BLM in the telomere maintenance pathways of ALT, telomerase positive and/or primary cells has not yet been established.

Here we report observations supporting a role for BLM in the human ALT pathway. We find that the BLM protein co-localizes with telomeric foci in ALT but not in telomerase positive or primary cell lines. We use fluorescent resonance energy transfer (FRET) and co-immunoprecipitation to provide evidence of intimate *in vivo* associations between BLM and the telomeric protein TRF2 in ALT cell lines. Overexpression of GFP–BLM results in rapid, ALT-specific accumulation of telomeric DNA, which is dependent on BLM helicase activity. Our observations suggest a functional role for BLM in ALT telomere maintenance, which may be mediated by interactions with TRF2.

RESULTS

Co-localization of BLM and telomeric foci in ALT cell lines

Dual indirect immunofluorescence staining with either of two anti-BLM antibodies detected BLM protein organized into multiple nuclear foci in the ALT cell lines WI38–VA13/2RA and GM00847 (Fig. 1). Antibodies raised against the human TRF1 protein were used to identify telomeric foci in these cells. The majority of BLM foci co-localized with telomeric foci in ~70% of cells in asynchronous cultures. This behavior is restricted to ALT cells, as individual BLM and telomeric foci rarely overlapped in telomerase-positive (GM00639 and AG10076) and primary cell lines (WI38 and GM01161; Fig. 1). These results were confirmed using antibodies raised against the human TRF2 protein to identify telomeric foci (data not shown).

In order to examine the frequency of co-localization between BLM, PML and telomeric foci in ALT cells, we transfected WI38–VA13/2RA with GFP–BLM and stained the cells with rabbit anti-PML and mouse anti-TRF1 antibodies (Fig. 2). Similar to previous observations (15) we observed that ~10% of cells exhibited PML bodies with large aggregates of TRF1 foci, however we also found ~60% of cells contained smaller TRF1 foci that co-localized with PML. We found that GFP–BLM co-localized with TRF1 in ~75% of cells and this co-localization occurred within PML bodies (Fig. 2). In contrast, GFP–BLM^{Q672R}, which has a missense mutation found in Bloom syndrome patients that inactivates the helicase domain (35), showed a more diffuse staining pattern with foci that co-localized with telomeric foci and PML bodies in only 7–9% of cells. These significant reductions in co-localization ($P < 0.01$, *t*-test) indicate that a functional helicase domain is necessary for GFP–BLM to efficiently co-localize with telomeres in ALT-associated PML bodies. We also found that overexpression of GFP–BLM^{Q672R} resulted in a moderate reduction in the proportion of cells which exhibit TRF1 and PML co-localization, 56% compared with 84% in cells expressing GFP alone ($P = 0.049$, *t*-test).

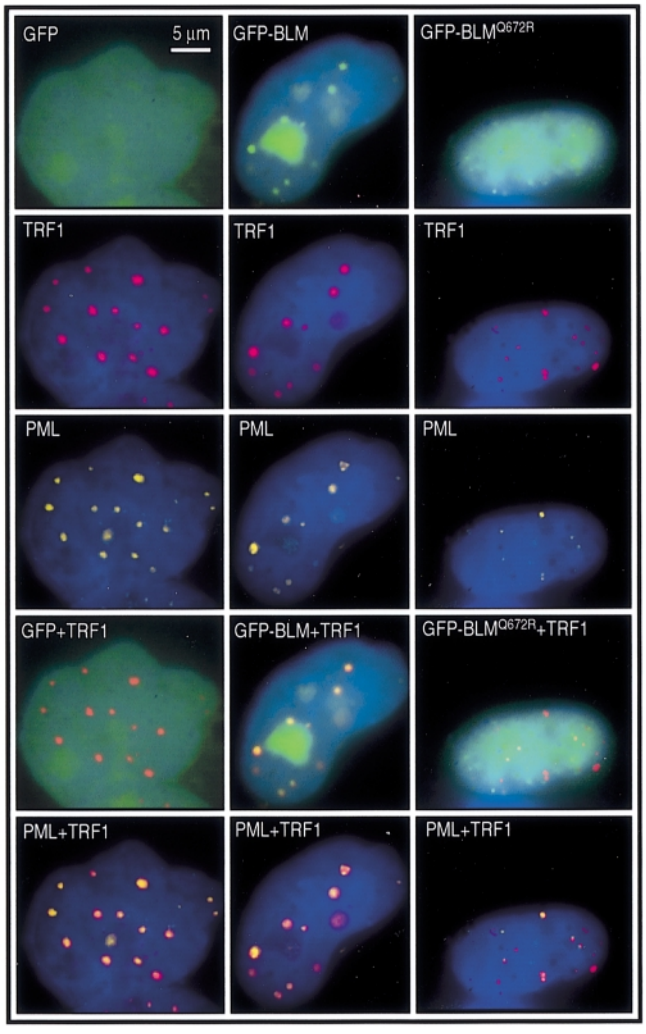

Figure 2. Intracellular localization of GFP-tagged BLM. WI38–VA13/2RA cells were transfected with GFP, GFP–BLM, or GFP–BLM^{Q672R} proteins (green) and stained with DAPI (blue), mouse anti-TRF1 (red) and rabbit anti-PML (yellow) 72 h post-transfection. Co-localization of GFP–BLM with telomeric foci occurs within PML bodies and is reduced by the Q672R point mutation. These results were obtained from two independent experiments in which 100 total cells were scored for each construct.

In vivo interactions between BLM and TRF2 proteins

To test for *in vivo* physical interactions between BLM and telomeric proteins we quantified FRET efficiency on WI38–VA13/2RA ALT cells that had been transfected with constructs that express BLM fused to cyan fluorescent protein (CFP–BLM) and the telomeric protein TRF2 fused to yellow fluorescent protein (YFP–TRF2). The acceptor molecules (YFP–TRF2) were photo-bleached and de-quenching of the donor molecules (CFP–BLM) were measured in nuclear regions where CFP–BLM and YFP–TRF2 foci co-localized (36). FRET efficiencies ranging from 6.5 to 14.5% (Fig. 3) were detected in ~10% of cells that showed co-localization between YFP–TRF2 and CFP–BLM ($n = 40$). These energy transfer efficiencies indicate less than 10 nm separation between YFP–TRF2 and CFP–BLM molecules (36) and imply that endogenous TRF2 and BLM directly interact at a subset of ALT telomeres. In contrast, no FRET was detected in WI38–VA13/2RA cells co-transfected with either CFP and YFP–TRF2 or YFP and CFP–BLM (not shown). In order to confirm *in vivo* interactions between BLM and TRF2 proteins, we performed co-immunoprecipitation experiments on GM00847 cells transiently expressing YFP–TRF2 (Fig. 3C). YFP–TRF2 was co-immunoprecipitated with an anti-BLM antibody, but not with an antibody specific for *Schistosoma japonicum* glutathione *S*-transferase (*sj*GST). These results confirm the FRET analysis that BLM and TRF2 proteins interact in ALT cells.

Effects of BLM overexpression on telomeric DNA content

We performed a quantitative measurement of total telomeric DNA content by fluorescent *in situ* hybridization followed by analysis on a fluorescence activated cell sorter (FLOW FISH) on ALT (GM00847) cells overexpressing GFP, GFP–BLM or GFP–BLM^{Q672R}. Since we were unable to establish long-term clones of cells overexpressing high levels of GFP–BLM or GFP–BLM^{Q672R}, we performed telomere fluorescence analysis on transiently transfected polyclonal populations of cells, which were sorted for GFP expression 60 h post-transfection. Telomere fluorescence analysis was performed on cells in the G1 phase of the cell cycle. The mean telomere fluorescence of G1 phase GM00847 cells expressing GFP-tagged BLM was 3-fold greater than cells expressing GFP alone, in three independent experiments ($307 \pm 19\%$), (Fig. 4A versus B; $Z = -14.4$, $P < 0.0001$, Mann–Whitney rank test). The variance in telomere fluorescence for GFP–BLM-positive cells was four times that of GFP-positive cells, due in large part to a marked increase in the proportion of cells with greater than twice the mean telomere fluorescence (23.3% of the GFP–BLM-positive cells versus 2.14% of the GFP-positive cells). Expression of GFP–BLM^{Q672R} had little effect, as the

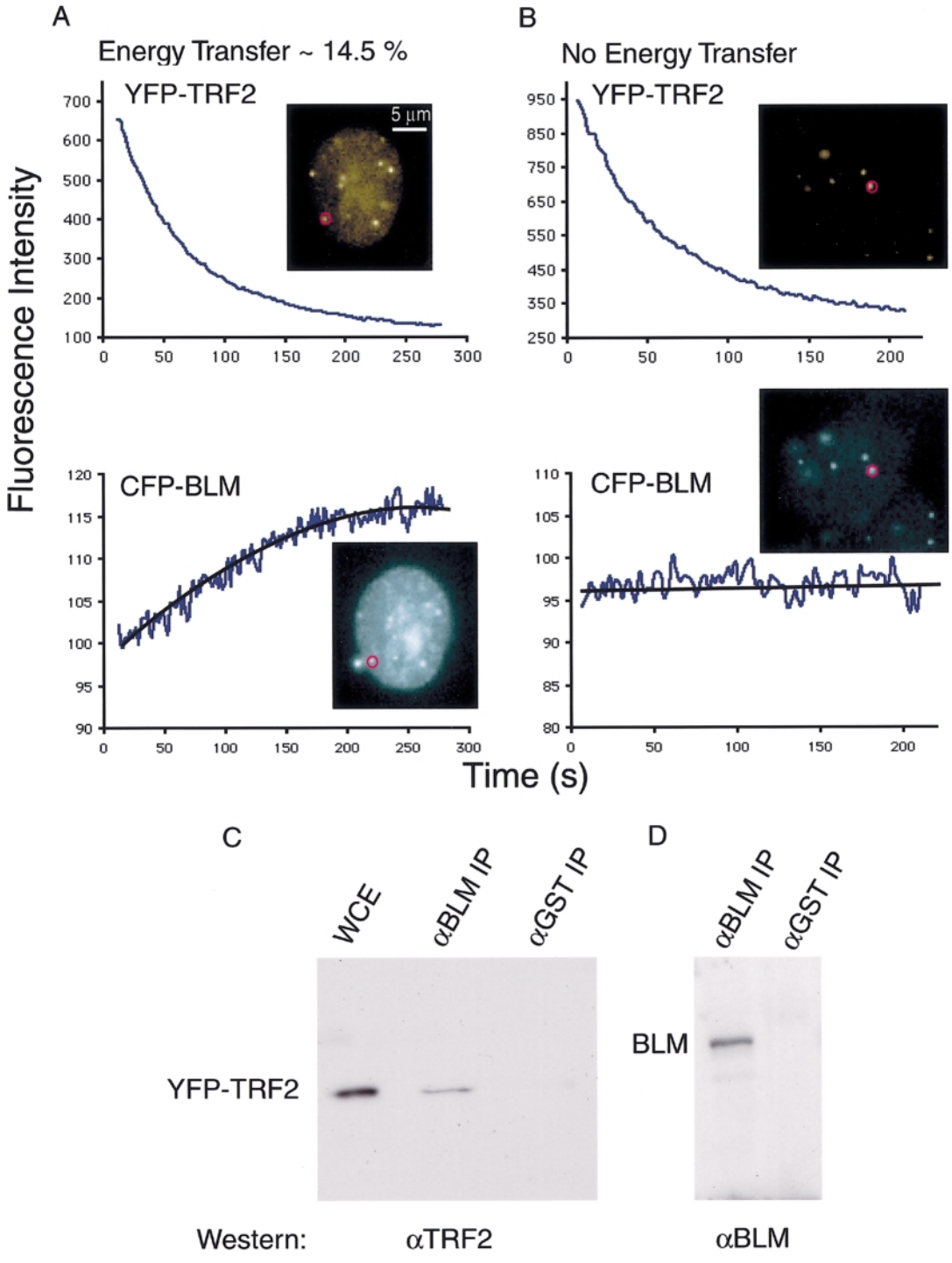

Figure 3. FRET and co-immunoprecipitation experiments show direct *in vivo* associations between BLM and TRF2 proteins in ALT cells. (**A**) WI38–VA13/2RA cells were co-transfected with CFP–BLM and YFP–TRF2. Expression of YFP–TRF2 in ALT cells results in foci, which co-localize with telomeric foci (not shown). FRET was measured at foci that exhibit co-localization between the two fusion proteins by bleaching the acceptor molecules, YFP–TRF2 (yellow), and measuring the de-quenching of the donor, CFP–BLM (cyan). The graph depicts the fluorescence intensity of YFP–TRF2 and CFP–BLM foci (circled in red), as the YFP–TRF2 molecules are photo-bleached. The FRET efficiency was determined using the equation $1 - I_a/I_b$, where I_a is the average of the first five fluorescence intensity readings of CFP-BLM, and I_b represents the final five readings of CFP–BLM intensity after the YFP–TRF2 was photo-bleached completely. An example of FRET with ~14.5% energy transfer between CFP–BLM and YFP–TRF2 is shown. Photo-bleaching of YFP–TRF2 in the focus circled in red caused coordinate increases in the focus' CFP-BLM fluorescence and decreases in its YFP–TRF2 fluorescence. (**B**) No energy transfer was observed in the circled foci, which co-localize. (**C**) Cell lysates from GM00847 expressing YFP–TRF2 were incubated with anti-BLM or anti-*sj*GST antibodies followed by western blot analysis with anti-TRF2 antibodies. Lane 1 shows YFP–TRF2 from whole cell extracts, which was co-immunoprecipitated by anti-BLM antibodies (lane 2) but not anti-*sj*GST antibodies (lane 3). (**D**) Western blot analysis showing immunoprecipitation of endogenous BLM with anti-BLM but not anti-*sj*GST antibodies. Similar co-immunoprecipitation experiments with GM00847 overexpressing YFP showed no evidence of interaction between BLM and the YFP moiety itself (data not shown).

mean telomere fluorescence was 85 ± 9% of GFP-expressing controls (Fig. 4A versus C). These results indicate that rapid increases in telomeric DNA synthesis are stimulated by overexpression of GFP–BLM and this effect is dependent on BLM helicase activity. Similar results were obtained with WI38–VA13/2RA (data not shown).

In order to verify the rapid increase in telomere DNA accumulation detected by FLOW FISH, GM00847 expressing GFP, GFP–BLM and GFP–BLM^{Q672R} were fixed onto microscope slides and hybridized with a telomere specific peptide nucleic acid (PNA) probe (Fig. 4G and H and data not shown). A subset of the GFP-expressing ALT cells (∼5%) contained large aggregates of telomeric DNA in interphase nuclei, as previously published (15). The proportion of GFP–BLM expressing cells with large aggregates of telomeric DNA was 32%, a 6-fold increase over that seen in the GFP-expressing cells. The fluorescence intensity of the large foci of telomeric DNA in GFP–BLM-expressing cells was often 10–20-fold greater than the brightest foci in GFP-expressing cells, while GFP–BLM^{Q672R}-expressing cells were similar to GFP-expressing cells (Fig. 4G and H and data not shown). These observations are consistent with the FLOW FISH data, as they show that overexpression of GFP–BLM results in a rapid accumulation of telomeric DNA, a phenomenon that is dependent on helicase activity.

The effect of GFP–BLM expression on telomere repeat synthesis was also examined in GM00639 cells. As expected for this telomerase-positive cell line (5), the mean and variance of cellular telomere DNA content of GFP-expressing GM00639 cells were smaller than those for GFP-expressing ALT cells (e.g. Fig. 4A versus D). In contrast to its effect on GM00847 ALT cells, overexpression of GFP–BLM had little effect on telomere fluorescence in GM00639 cells in three independent experiments (119 ± 15%, Fig. 4D versus E). Finally, similar to ALT cells, overexpression of GFP–BLM^{Q672R} in GM00639 cells exhibited a slight reduction of telomere fluorescence (87 ± 6% of GFP transfected controls; Fig. 4F).

DISCUSSION

We have shown by immunofluorescence studies that the BLM protein co-localizes with telomeric foci in ∼70% of cells in asynchronous cultures of ALT human cell lines. This high degree of co-localization is specific to cells that maintain their telomeres by ALT, as it was not seen in telomerase-positive or primary human cells. Our results are consistent with a previous study (33), which found frequent BLM-TRF1 co-localization in telomerase-negative GM00637 immortalized fibroblasts but only occasional overlap of individual foci in WI38 primary fibroblasts.

BLM co-localizes with PML bodies in ∼85% of unsynchronized HeLa cells, and ∼90% of BLM foci overlap with PML foci in these cells (21). It has previously been reported that PML bodies co-localize with large aggregates of TRF1 in only ∼5% of asynchronously growing human ALT cells (15), yet in our studies BLM co-localized with telomeric foci in ∼70% of asynchronous cultures of ALT cells. Therefore, we investigated whether BLM–TRF1 co-localization occurred outside of the PML nuclear domains in ALT cells. Our analysis of PML–TRF1 co-localization in WI38–VA13/2RA showed that PML protein co-localized with TRF1 in ∼75% of cells. Approximately 5–10% of cells exhibited large aggregates of TRF1 co-localizing with PML protein (Fig. 2, data not shown), however we also found that smaller telomeric foci co-localized with PML in about 60% of cells. Other laboratories have shown that 10–30% (37) and 50–60% (38) of asynchronously growing ALT cells exhibit co-localization between TRF2 and PML protein. The differences are likely to be due to different cell fixation methods and/or antibodies used to detect PML and/or telomeric proteins. For example, our fixation methodology results in greater access of the antibody to nuclear proteins (see Materials and Methods) and the polyclonal antibody we used to detect PML protein (AB1370, Chemicon) provides a stronger signal by immunofluorescence when compared with the more commonly used monoclonal antibody PG-M3 (Santa Cruz; data not shown). GFP–BLM co-localized with telomeric foci almost exclusively within PML nuclear domains. Thus, the association we observed between BLM and telomeric foci in ALT cell lines occurs predominately within PML nuclear domains. The moderate decrease in the proportion of cells exhibiting co-localization between PML and TRF1 following expression of GFP–BLM^{Q672R} suggests an inhibitory effect on the formation of APBs.

The telomeric protein, TRF2, maintains the structural integrity of human telomeres (39), and probably prevents their recognition as double strand breaks by catalyzing formation of protective t-loops (40,41). We found evidence for direct interaction between human BLM and TRF2 *in vivo* by FRET analysis and co-immunoprecipitations. The detection of FRET in only 10% of foci where CFP–BLM and YFP–TRF2 co-localize suggests that direct physical interaction between BLM and TRF2 may be transient (Fig. 3B). For example, it is possible that BLM may only associate with TRF2 during the initial stages of telomere elongation by ALT (see later and Fig. 4A). Furthermore, the co-localization of BLM with telomeres in the majority of ALT cells may represent interactions with other telomere components including telomeric DNA, TRF1 or proteins involved in homologous recombination and DNA replication during ALT telomere elongation.

Our finding that overexpression of the BLM helicase leads to rapid, ALT cell-specific, increases in telomeric DNA synthesis indicates that the human ALT pathway of telomere maintenance is selectively up-regulated by overexpression of a functional BLM helicase. These results lend support to previous observations that the ALT pathway is repressed in telomerase-positive immortalized cell lines (42). The BLM homolog, Sgs1, has been recently shown to be required for the type II ALT pathway in *S. cerevisiae*, which exhibits a similar telomere length profile to human ALT cell lines (43–45). Taken together, these observations implicate a conserved role for the RecQ sub-family of DNA helicases in ALT telomere maintenance between *S. cerevisiae* and humans.

The precise role played by recombination in ALT lengthening of telomeres is unknown. Both break-induced replication and rolling circle amplification have been proposed as mechanisms through which telomeres are elongated in yeast that lack telomerase (13,46,47). We favor the latter model to explain the abrupt, 10–20-fold increases in nuclear telomeric DNA seen in

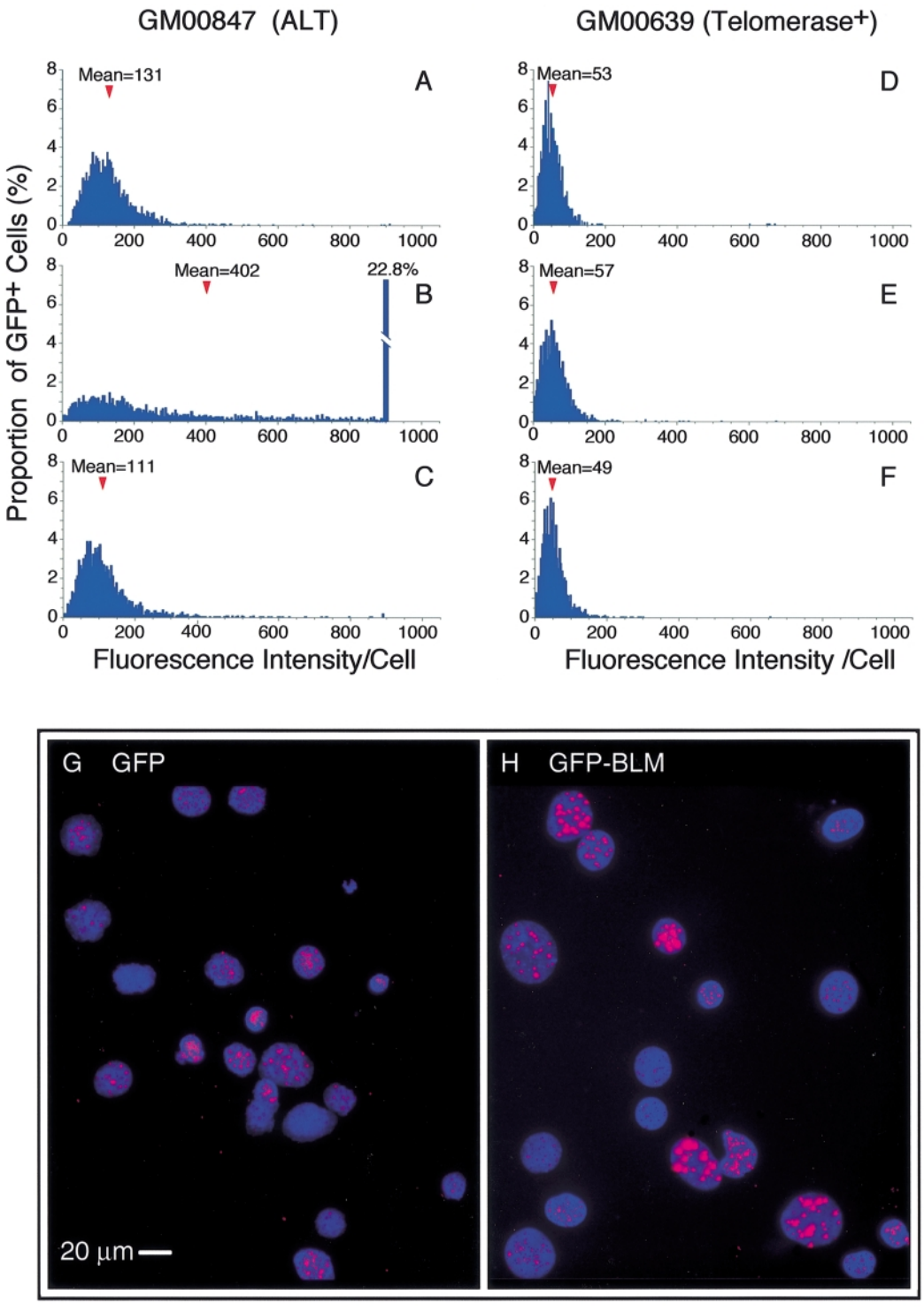

Figure 4. Flow FISH analysis of cells expressing GFP, GFP–BLM and GFP–BLM^{Q672R}. GM00847 and GM00639 were transfected with GFP (**A** and **D**), GFP–BLM (**B** and **E**) or GFP–BLM^{Q672R} (**C** and **F**), followed by telomere fluorescence analysis of cells in G1 phase of the cell cycle by FLOW FISH, 60 h post-transfection. The mean telomere fluorescence/cell for each population was calculated by subtracting the mean background fluorescence and is indicated above each histogram. These histograms are representative of three independent experiments that showed similar results. All cells with fluorescence intensities greater than the maximum values detected by the flow cytometer were counted in the highest fluorescence value column in the histogram. GM00847 expressing GFP (**G**), GFP-BLM (**H**) and GFP-BLM^{Q672R} (not shown) were hybridized with a rhodamine-conjugated telomere-specific PNA probe and observed with a fluorescence microscope to confirm the presence of nuclei with exceptionally high telomere fluorescence in GFP–BLM transfected cells. In order to quantitatively compare fluorescence intensities between samples, we used exposure times that maintained the fluorescence values of the brightest telomeric foci within the linear range of the digital camera. Figures shown here (**G** and **H**) were taken at exposure times which exceeded the linear range of the camera for the brightest foci, but allowed visualization of less intense telomeric foci in the same image as the brightest foci. Note a higher proportion of BLM-expressing cells have large telomeric foci, many of which are much brighter than the brightest foci from GFP-expressing nuclei.

less than three cell divisions after transfection of ALT cells with GFP–BLM. Telomerase-deficient *Kluyveromyces lactis* yeast have been shown to be capable of elongating their telomeres using extra-chromosomal circular DNAs containing telomeric repeat sequences as templates (48). Extra-chromosomal DNA has been found in ALT cell lines and small polydisperse circular telomeric DNA has been detected in some tumors and immortalized cell lines (8–10). The latter could be used as a template in a rolling-circle amplification scheme that is facilitated by high-level expression of GFP–BLM. Alternatively, overexpression of GFP–BLM may promote an intra-chromosomal rolling-circle process that utilizes the t-loop structure shown in Figure 5A and B. GFP–BLM overexpression may also drive amplification of extrachromosomal circular telomeric DNAs in ALT cells, a possibility that is under active investigation.

Our results identify BLM as the first protein found to affect telomeric DNA synthesis specifically in human ALT immortalized cell lines. The *in vivo* association we detected between YFP–TRF2 and CFP–BLM in ALT cells suggest that BLM and TRF2 may co-operate in telomere elongation. The *Escherichia coli* BLM homolog RecQ promotes the ability of RecA to carry out strand invasion and D-loop formation *in vitro* (49). Similarly, the ability of BLM helicase to unwind DNA with 3′ overhangs (50) and to enlarge internal bubbles in double-stranded DNA (51) may allow it to help TRF2 initiate and extend strand invasion between telomeric sequences (Fig. 5A), a common first step in the recombination-dependent pathways of telomere elongation outlined above. Our observations that BLM is at telomeric foci in a majority of ALT cells but that direct interactions between CFP–BLM and YFP–TRF2 occur in only a minority of these foci suggest that BLM plays additional, TRF2-independent, roles in ALT. For example, once rolling-circle replication begins, BLM may facilitate telomere elongation by: (1) unwinding duplex DNA and G4 structures (27) in advance of the replication fork (C in Fig. 5B); and/or (2) promoting branch migration of the Holiday junction (30) formed behind the replication fork (D in Fig. 5B).

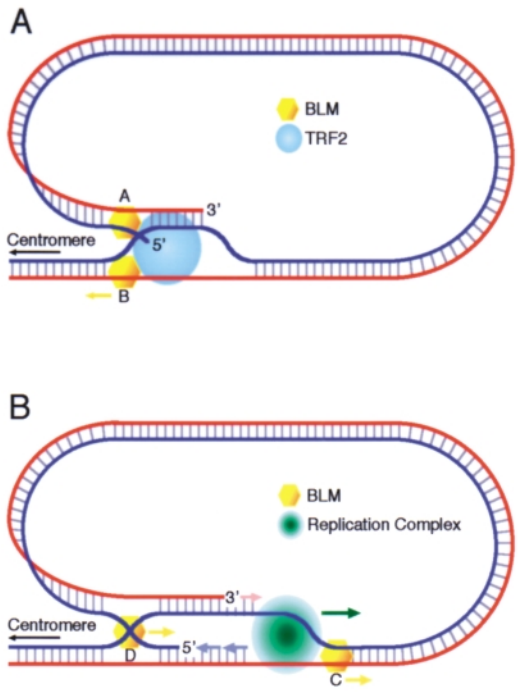

Figure 5. A model for rolling-circle amplification of telomeres. In this model, BLM and TRF2 co-operate in forming a t-loop in which both the 3′ and 5′ ends of the telomere pair with their complementary strands at the base of the t-loop so as to form a four-stranded rolling circle (**A**). The replication machinery then adds to both strands of the telomere end using the base's strands as templates. Subsequent branch migration of the Holiday junction that forms behind the replication machinery allows for continuous replication of the rolling circle and results in extensive lengthening of the telomere (**B**). Possible roles for the BLM helicase include unwinding the free end of the telomere (A) and expanding bubbles in the double-stranded recipient DNA during formation of the t-loop (B), unwinding DNA ahead of the replication fork (C), and promoting branch migration of the Holiday junction behind the replication fork (D). While an intra-telomeric loop is illustrated, this scheme also can apply to the use of extra-chromosomal circles of telomeric DNA as the template.

MATERIALS AND METHODS

Cell culture and transfections

WI38 (primary fibroblasts) and WI38–VA13/2RA (SV40-transformed fibroblasts; telomerase negative) were obtained from the American Type Culture Collection. GM01161 primary fibroblasts and the SV40 transformed fibroblasts GM00847 (telomerase negative), GM00639 (telomerase positive) and AG10076 (telomerase positive) were obtained from the Coriell Institute for Medical Research. Transfections were carried out with either Effectene (Qiagen) or Fugene 6 (RocheDiagnostics) transfection reagents as instructed by the manufacturers.

Plasmids

The GFP–BLM expression construct was obtained from Dr N.A. Ellis and is described elsewhere (52). GFP–BLM^{Q672R} was constructed by cloning the *Xmn*I and *Sal*I fragment from the BLM^{Q672R} cDNA obtained from Dr N.A. Ellis (35) into the GFP–BLM expression construct. The TRF2 cDNA was cloned by screening an oligo-dT primed cDNA library of the colon carcinoma-derived cell line, Caco-2 (ATCC cell line HTB36) with a radio-labeled probe corresponding to the 5′ end of hTRF2, using standard methods (53). Inserts of positive clones were excised as recommended by the supplier of the Uni-ZAPTM XR vector (Stratagene) used to prepare the library and sequenced for verification. The TRF2 cDNA was then cloned in-frame into the pEYFP-C1 plasmid and sequenced (Clontech).

Immunofluorescence

Cells were grown on chamber slides (Falcon), rinsed with PBS, fixed with 2% paraformaldehyde and 0.2% Triton X-100 in dH_2O (pH 8.2) for 20 min at room temperature (RT) and rinsed 3×5 min with PBS. Immunostaining was carried out as described previously (54). Primary antibodies, mouse or rabbit anti-TRF1 (55) were used to identify telomeric foci; rabbit anti-BLM (56) or mouse anti-BLM (BFL103) (57) were used for BLM localization; and rabbit anti-PML (Ab1370, Chemicon) identified PML protein. Secondary antibodies, fluore-

scein isothiocyanate-conjugated donkey anti-rabbit, Cyan 5-conjugated donkey anti-rabbit, and tetramethyl rhodamine isothiocyanate-conjugated donkey anti-mouse were obtained from Jackson ImmunoResearch Laboratories (West Grove, PA, USA). WI38–VA13/2RA was transfected with GFP, GFP–BLM or GFP–BLM^{Q672R} with Effectene (Qiagen) and fixed 72 h post-transfection for immunofluorescence analysis. DNA was stained with 4′,6-diamido-2-phenylindole (0.2 μg/ml) in PBS. Images were obtained using a 60× 1.4 NA objective mounted onto a Nikon Eclipse E1000 microscope equipped with a Princeton Instruments Micromax camera with 15 μM square pixels. IP lab (Scanalytics) was used to acquire 12 bit gray-scale images from the camera, which were subsequently merged into 8 bit color images with Adobe Photoshop.

FRET analysis

The BLM cDNA was cloned into the pECFP-C1 plasmid (Clontech) and co-transfected with YFP–TRF2 into WI38–VA13/2RA cells using Effectene (Qiagen). Cells were imaged at 22°C 48–72 h post-transfection on an Olympus IX70 microscope with a CCD camera (MicroMax 1300YHS) controlled by MetaFluor 4.5r2 software (Universal Imaging). Acceptor bleaching of YFP–TRF2 and CFP–BLM was performed using a 510DF23 excitation filter and a 450–520–590TBDR dichromic mirror. The intensities of CFP and YFP were measured with a 440DF20 excitation filter and 480DF30 emission filter (CFP) and a 510DF23 excitation filter and 535DF25 emission filter (YFP), alternated by a filter changer (Lambda 10-2, Sutter Instruments). Interference filters were obtained from Omega Optical.

Immunoprecipitations and western analysis

GM00847 cells were transfected with the YFP–TRF2 construct and approximately 5×10^6 cells in 500 μl lysis buffer were used for each experiment. Whole cell extracts were prepared 48 h post-transfection as described previously (57). Extracts were incubated with anti-BLM at 1 : 1500 (NB 100-161, Novus-Biologicals) or anti-*sj*GST at 1 : 1500 (Z-5, Santa Cruz) for 1 h, followed by protein G sepharose beads (Amersham Pharmacia) for 6 h at 4°C. The beads were collected by centrifugation and were washed for 4 × 10 min at 4°C with 1 ml lysis buffer. The immunocomplexes were boiled in 40 μl Lamelli buffer. Samples were separated on a 7.5% SDS–PAGE and transferred to PVDF membrane by standard methods. The immunoblots were blocked with 5% milk powder in PBS for 2 h at RT, and incubated with mouse monoclonal anti-TRF2 antibody at 1 : 250 (IMG-124, IMGENEX) in Tris-buffered saline with 0.1% Tween 20 (TBST) for 2 h at RT. The blots were washed 3 × 10 min with TBST at RT and incubated with horseradish peroxidase conjugated donkey anti-mouse at 1 : 10 000 (Jackson ImmunoResearch Laboratories) for 1 h at RT. Western blot analysis of immunoprecipitates to detect BLM was performed as above except that samples were separated on a 5% SDS–PAGE gel, blots were incubated with anti-BLM (NB 100-61, Novus Biologicals) at 1 : 3000 and protein A-conjugated HRP (Sigma) at 1 : 5000. Chemiluminescent detection was performed using ECL.

FLOW FISH

GM00847 and GM00639 were transfected with GFP, GFP–BLM, GFP–BLM^{Q672R} constructs using Fugene 6 (Roche) and GFP-positive cells were sorted 60 h post-transfection using an Epics Elite (Beckman Coulter) fluorescence activated cell sorter. Flow FISH was performed as described previously (58) except that the denaturation step was performed at 86°C for 10 min and DNA was stained with 7-amino actinomycin D (1 mg/ml). Cells were analysed using a FACScan flow cytometer (Becton Dickinson) with Cell Quest software. Telomere fluorescence/cell was calculated from cells in the G1 phase of the cell cycle gated on DNA content. The mean of telomere fluorescence for each sample was corrected for background fluorescence using control hybridizations without PNA telomeric probe. For microscope analysis of telomere fluorescence in interphase nuclei, GFP-sorted cells were hybridized with a rhodamine-conjugated telomeric PNA probe as previously described (59). Images were acquired using an axioplan 2 epi-fluorescence microscope (Zeiss) using a 20× Plan-APOCHROMAT (Zeiss) lens and Orca ER CCD camera (Hamamatsu) with OPENLAB 3.0.4 software (Improvision).

ACKNOWLEDGEMENTS

We greatly appreciate the donations of antibodies from T. de Lange, I.D. Hickson and H. Youssoufian and the generous advice provided by J. Rommens, L. Harrington and E. Arpaia. We also thank N.A. Ellis for cDNA constructs and J. Rommens for the cDNA library. This work was supported by a National Cancer Institute (Canada) operating grant to M.S.M., Canadian Institutes for Health Research Fellowship to M.U., I.P and K.T. and an Ontario Graduate Scholarship and Hospital for Sick Children Research Institute Fellowship to D.J.S.

REFERENCES

1. Counter, C.M., Avilion, A.A., LeFeuvre, C.E., Stewart, N.G., Greider, C.W., Harley, C.B. and Bacchetti, S. (1992) Telomere shortening associated with chromosome instability is arrested in immortal cells which express telomerase activity. *EMBO. J.*, **11**, 1921–1929.
2. Kim, N.W., Piatyszek, M.A., Prowse, K.R., Harley, C.B., West, M.D., Ho, P.L., Coviello, G.M., Wright, W.E., Weinrich, S.L. and Shay, J.W. (1994) Specific association of human telomerase activity with immortal cells and cancer. *Science*, **266**, 2011–2015.
3. Counter, C.M., Hirte, H.W., Bacchetti, S. and Harley, C.B. (1994) Telomerase activity in human ovarian carcinoma. *Proc. Natl Acad. Sci. USA*, **91**, 2900–2904.
4. Murnane, J.P., Sabatier, L., Marder, B.A. and Morgan, W.F. (1994) Telomere dynamics in an immortal human cell line. *EMBO. J.*, **13**, 4953–4962.
5. Bryan, T.M., Englezou, A., Gupta, J., Bacchetti, S. and Reddel, R.R. (1995) Telomere elongation in immortal human cells without detectable telomerase activity. *EMBO. J.*, **14**, 4240–4248.
6. Bryan, T.M., Englezou, A., Dalla-Pozza, L., Dunham, M.A. and Reddel, R.R. (1997) Evidence for an alternative mechanism for maintaining telomere length in human tumors and tumor-derived cell lines. *Nat. Med.*, **3**, 1271–1274.
7. Bryan, T.M., Marusic, L., Bacchetti, S., Namba, M. and Reddel, R.R. (1997) The telomere lengthening mechanism in telomerase-negative immortal human cells does not involve the telomerase RNA subunit. *Hum. Mol. Genet.*, **6**, 921–926.

8. Ogino, H., Nakabayashi, K., Suzuki, M., Takahashi, E., Fujii, M., Suzuki, T. and Ayusawa, D. (1998) Release of telomeric DNA from chromosomes in immortal human cells lacking telomerase activity. *Biochem. Biophys. Res. Commun.*, **248**, 223–227.
9. Regev, A., Cohen, S., Cohen, E., Bar-Am, I. and Lavi, S. (1998) Telomeric repeats on small polydisperse circular DNA (spcDNA) and genomic instability. *Oncogene*, **17**, 3455–3461.
10. Tokutake, Y., Matsumoto, T., Watanabe, T., Maeda, S., Tahara, H., Sakamoto, S., Niida, H., Sugimoto, M., Ide, T. and Furuichi, Y. (1998) Extra-chromosomal telomere repeat DNA in telomerase-negative immortalized cell lines. *Biochem. Biophys. Res. Commun.*, **247**, 765–772.
11. Lundblad, V. and Blackburn, E.H. (1993) An alternative pathway for yeast telomere maintenance rescues est1- senescence. *Cell*, **73**, 347–360.
12. Friedberg, E.C. (1988) Deoxyribonucleic acid repair in the yeast *Saccharomyces cerevisiae. Microbiol. Rev.*, **52**, 70–102.
13. Le, S., Moore, J.K., Haber, J.E. and Greider, C.W. (1999) RAD50 and RAD51 define two pathways that collaborate to maintain telomeres in the absence of telomerase. *Genetics*, **152**, 143–152.
14. Teng, S.C. and Zakian, V.A. (1999) Telomere-telomere recombination is an efficient bypass pathway for telomere maintenance in Saccharomyces cerevisiae. *Mol. Cell. Biol.*, **19**, 8083–8093.
15. Yeager, T.R., Neumann, A.A., Englezou, A., Huschtscha, L.I., Noble, J.R. and Reddel, R.R. (1999) Telomerase-negative immortalized human cells contain a novel type of promyelocytic leukemia (PML) body. *Cancer Res.*, **59**, 4175–4179.
16. Wu, G., Lee, W.H. and Chen, P.L. (2000) NBS1 and TRF1 colocalize at promyelocytic leukemia bodies during late S/G2 phases in immortalized telomerase-negative cells. Implication of NBS1 in alternative lengthening of telomeres. *J. Biol. Chem.*, **275**, 30618–30622.
17. Seeler, J.S. and Dejean, A. (1999) The PML nuclear bodies: actors or extras? *Curr. Opin. Genet. Devl.*, **9**, 362–367.
18. Quignon, F., De Bels, F., Koken, M., Feunteun, J., Ameisen, J.C. and de The, H. (1998) PML induces a novel caspase-independent death process. *Nat. Genet.*, **20**, 259–265.
19. Wang, Z.G., Ruggero, D., Ronchetti, S., Zhong, S., Gaboli, M., Rivi, R. and Pandolfi, P.P. (1998) PML is essential for multiple apoptotic pathways. *Nat. Genet.*, **20**, 266–272.
20. Wang, Z.G., Delva, L., Gaboli, M., Rivi, R., Giorgio, M., Cordon-Cardo, C., Grosveld, F. and Pandolfi, P.P. (1998) Role of PML in cell growth and the retinoic acid pathway. *Science*, **279**, 1547–1551.
21. Zhong, S., Hu, P., Ye, T.Z., Stan, R., Ellis, N.A. and Pandolfi, P.P. (1999) A role for PML and the nuclear body in genomic stability. *Oncogene*, **18**, 7941–7947.
22. Carbone, R., Pearson, M., Minucci, S. and Pelicci, P.G. (2002) PML NBs associate with the hMre11 complex and p53 at sites of irradiation induced DNA damage. *Oncogene*, **21**, 1633–1640.
23. Bischof, O., Kim, S.H., Irving, J., Beresten, S., Ellis, N.A. and Campisi, J. (2001) Regulation and localization of the Bloom syndrome protein in response to DNA damage. *J. Cell. Biol.*, **153**, 367–380.
24. Dunham, M.A., Neumann, A.A., Fasching, C.L. and Reddel, R.R. (2000) Telomere maintenance by recombination in human cells. *Nat. Genet.*, **26**, 447–450.
25. Ellis, N.A., Groden, J., Ye, T.Z., Straughen, J., Lennon, D.J., Ciocci, S., Proytcheva, M. and German, J. (1995) The Bloom's syndrome gene product is homologous to RecQ helicases. *Cell*, **83**, 655–666.
26. Johnson, F.B., Lombard, D.B., Neff, N.F., Mastrangelo, M.A., Dewolf, W., Ellis, N.A., Marciniak, R.A., Yin, Y., Jaenisch, R. and Guarente, L. (2000) Association of the Bloom syndrome protein with topoisomerase IIIalpha in somatic and meiotic cells. *Cancer Res.*, **60**, 1162–1167.
27. van Brabant, A.J., Ye, T., Sanz, M., German, I.J., Ellis, N.A. and Holloman, W.K. (2000) Binding and melting of D-loops by the Bloom syndrome helicase. *Biochemistry*, **39**, 14617–14625.
28. Wu, L., Davies, S.L., Levitt, N.C. and Hickson, I.D. (2001) Potential role for the BLM helicase in recombinational repair via a conserved interaction with RAD51. *J. Biol. Chem.*, **276**, 19375–19381.
29. Walpita, D., Plug, A.W., Neff, N.F., German, J. and Ashley, T. (1999) Bloom's syndrome protein, BLM, colocalizes with replication protein A in meiotic prophase nuclei of mammalian spermatocytes. *Proc. Natl Acad. Sci. USA*, **96**, 5622–5627.
30. Karow, J.K., Constantinou, A., Li, J.L., West, S.C. and Hickson, I.D. (2000) The Bloom's syndrome gene product promotes branch migration of holiday junctions. *Proc. Natl Acad. Sci. USA*, **97**, 6504–6508.
31. Sun, H., Karow, J.K., Hickson, I.D. and Maizels, N. (1998) The Bloom's syndrome helicase unwinds G4 DNA. *J. Biol. Chem.*, **273**, 27587–27592.
32. German, J. (1993) Bloom syndrome: a mendelian prototype of somatic mutational disease. *Medicine (Baltimore)*, **72**, 393–406.
33. Yankiwski, V., Marciniak, R.A., Guarente, L. and Neff, N.F. (2000) Nuclear structure in normal and Bloom syndrome cells. *Proc. Natl Acad. Sci. USA*, **97**, 5214–5219.
34. Ishov, A.M., Sotnikov, A.G., Negorev, D., Vladimirova, O.V., Neff, N., Kamitani, T., Yeh, E.T., Strauss, J.F., III and Maul, G.G. (1999) PML is critical for ND10 formation and recruits the PML-interacting protein daxx to this nuclear structure when modified by SUMO-1. *J. Cell. Biol.*, **147**, 221–234.
35. Neff, N.F., Ellis, N.A., Ye, T.Z., Noonan, J., Huang, K., Sanz, M. and Proytcheva, M. (1999) The DNA helicase activity of BLM is necessary for the correction of the genomic instability of bloom syndrome cells. *Mol. Biol. Cell*, **10**, 665–676.
36. Miyawaki, A. and Tsien, R.Y. (2000) Monitoring protein conformations and interactions by fluorescence resonance energy transfer between mutants of green fluorescent protein. *Meth. Enzymol.*, **327**, 472–500.
37. Grobelny, J.V., Kulp-McEliece, M. and Broccoli, D. (2001) Effects of reconstitution of telomerase activity on telomere maintenance by the alternative lengthening of telomeres (ALT) pathway. *Hum. Mol. Genet.*, **10**, 1953–1961.
38. Cerone, M.A., Londono-Vallejo, J.A. and Bacchetti, S. (2001) Telomere maintenance by telomerase and by recombination can coexist in human cells. *Hum. Mol. Genet.*, **10**, 1945–1952.
39. van Steensel, B., Smogorzewska, A. and de Lange, T. (1998) TRF2 protects human telomeres from end-to-end fusions. *Cell*, **92**, 401–413.
40. Griffith, J.D., Comeau, L., Rosenfield, S., Stansel, R.M., Bianchi, A., Moss, H. and de Lange, T. (1999) Mammalian telomeres end in a large duplex loop. *Cell*, **97**, 503–514.
41. Karlseder, J., Broccoli, D., Dai, Y., Hardy, S. and de Lange, T. (1999) p53- and ATM-dependent apoptosis induced by telomeres lacking TRF2. *Science*, **283**, 1321–1325.
42. Perrem, K., Bryan, T.M., Englezou, A., Hackl, T., Moy, E.L. and Reddel, R.R. (1999) Repression of an alternative mechanism for lengthening of telomeres in somatic cell hybrids. *Oncogene*, **18**, 3383–3390.
43. Huang, P., Pryde, F.E., Lester, D., Maddison, R.L., Borts, R.H., Hickson, I.D. and Louis, E.J. (2001) SGS1 is required for telomere elongation in the absence of telomerase. *Curr. Biol.*, **11**, 125–129.
44. Johnson, F.B., Marciniak, R.A., McVey, M., Stewart, S.A., Hahn, W.C. and Guarente, L. (2001) The Saccharomyces cerevisiae WRN homolog Sgs1p participates in telomere maintenance in cells lacking telomerase. *EMBO. J.*, **20**, 905–913.
45. Cohen, H. and Sinclair, D.A. (2001) Recombination-mediated lengthening of terminal telomeric repeats requires the Sgs1 DNA helicase. *Proc. Natl Acad. Sci. USA*, **98**, 3174–3179.
46. Teng, S.C., Chang, J., McCowan, B. and Zakian, V.A. (2000) Telomerase-independent lengthening of yeast telomeres occurs by an abrupt Rad50p-dependent, Rif-inhibited recombinational process. *Mol. Cell.*, **6**, 947–952.
47. Bosco, G. and Haber, J.E. (1998) Chromosome break-induced DNA replication leads to nonreciprocal translocations and telomere capture. *Genetics*, **150**, 1037–1047.
48. Natarajan, S. and McEachern, M.J. (2002) Recombinational telomere elongation promoted by DNA circles. *Mol. Cell. Biol.*, **22**, 4512–4521.
49. Harmon, F.G. and Kowalczykowski, S.C. (1998) RecQ helicase, in concert with RecA and SSB proteins, initiates and disrupts DNA recombination. *Genes. Devl.*, **12**, 1134–1144.
50. Karow, J.K., Chakraverty, R.K. and Hickson, I.D. (1997) The Bloom's syndrome gene product is a 3′–5′ DNA helicase. *J. Biol. Chem.*, **272**, 30611–30614.
51. Mohaghegh, P., Karow, J.K., Brosh, R.M., Jr., Bohr, V.A. and Hickson, I.D. (2001) The Bloom's and Werner's syndrome proteins are DNA structure-specific helicases. *Nucleic Acids Res.*, **29**, 2843–2849.
52. Hu, P., Beresten, S.F., van Brabant, A.J., Ye, T.Z., Pandolfi, P.P., Johnson, F.B., Guarente, L. and Ellis, N.A. (2001) Evidence for BLM and topoisomerase III alpha interaction in genomic stability. *Hum. Mol. Genet.*, **10**, 1287–1298.
53. Sambrook, J., F.E.F.a.M.T. (1989) *Molecular Cloning: a Laboratory Manual.*, 2nd edn. Cold Spring Harbor Laboratory, Cold Spring Harbor, NY.

54. van Steensel, B. and de lange, T. (1997) Control of telomere length by the human telomeric protein TRF1. *Nature*, **385**, 740–743.
55. Zhu, X.D., Kuster, B., Mann, M., Petrini, J.H. and Lange, T. (2000) Cell-cycle-regulated association of RAD50/MRE11/NBS1 with TRF2 and human telomeres. *Nat. Genet.*, **25**, 347–352.
56. Gharibyan, V. and Youssoufian, H. (1999) Localization of the Bloom syndrome helicase to punctate nuclear structures and the nuclear matrix and regulation during the cell cycle: comparison with the Werner's syndrome helicase. *Mol. Carcinog.*, **26**, 261–273.
57. Wu, L., Davies, S.L., North, P.S., Goulaouic, H., Riou, J.F., Turley, H., Gatter, K.C. and Hickson, I.D. (2000) The Bloom's syndrome gene product interacts with topoisomerase III. *J. Biol. Chem.*, **275**, 9636–9644.
58. Rufer, N., Dragowska, W., Thornbury, G., Roosnek, E. and Lansdorp, P.M. (1998) Telomere length dynamics in human lymphocyte subpopulations measured by flow cytometry. *Nat. Biotechnol.*, **16**, 743–747.
59. Zijlmans, J.M., Martens, U.M., Poon, S.S., Raap, A.K., Tanke, H.J., Ward, R.K. and Lansdorp, P.M. (1997) Telomeres in the mouse have large inter-chromosomal variations in the number of T2AG3 repeats. *Proc. Natl Acad. Sci. USA*, **94**, 7423–7428.